AIP | Journal of Applied Physics

Effects of hydrogen plasma treatment on the electrical behavior of solution-processed ZnO transistors

Yesul Jeong, Christopher Pearson, Yong Uk Lee, Kyun Ahn, Chae-Ryong Cho, Jaeeun Hwang, Hongdoo Kim, Lee-Mi Do, and Michael C. Petty

Citation: Journal of Applied Physics **116**, 074509 (2014); doi: 10.1063/1.4893470
View online: http://dx.doi.org/10.1063/1.4893470
View Table of Contents: http://scitation.aip.org/content/aip/journal/jap/116/7?ver=pdfcov
Published by the AIP Publishing

Effects of hydrogen plasma treatment on the electrical behavior of solution-processed ZnO transistors

Yesul Jeong,[1] Christopher Pearson,[1] Yong Uk Lee,[2] Kyun Ahn,[3] Chae-Ryong Cho,[3] Jaeeun Hwang,[4] Hongdoo Kim,[4] Lee-Mi Do,[5] and Michael C. Petty[1,a)]
[1]*School of Engineering and Computing Sciences and Centre for Molecular and Nanoscale Electronics, Durham University, South Road, Durham DH1 3LE, United Kingdom*
[2]*Centre for Process Innovation Limited, Thomas Wright Way, Sedgefield, Durham TS21 3FG, United Kingdom*
[3]*Department of Nano Fusion Technology, Pusan National University, Miryang 627-706, Korea*
[4]*Department of Advanced Materials Engineering for Information and Electronics, Kyung Hee University, Yongin 446-701, Korea*
[5]*IT Convergence Technology Research Laboratory, Electronics and Telecommunications Research Institute, Daejeon 305-700, Korea*

(Received 31 May 2014; accepted 6 August 2014; published online 20 August 2014)

The effects of hydrogen plasma treatment on the active layer of top-contact zinc oxide thin film transistors are reported. The transfer characteristics of the reference devices exhibited large hysteresis effects and an increasing positive threshold voltage (V_{TH}) shift on repeated measurements. In contrast, following the plasma processing, the corresponding characteristics of the transistors exhibited negligible hysteresis and a very small V_{TH} shift; the devices also possessed higher field effect carrier mobility values. These results were attributed to the presence of functional groups in the vicinity of the semiconductor/gate insulator interface, which prevents the formation of an effective channel. [http://dx.doi.org/10.1063/1.4893470]

I. INTRODUCTION

In order to realize large-volume, flexible electronics, current research is directed at improving electronic transport by judicious choice of the semiconductor material, and at lowering processing temperatures by exploiting lower-cost manufacturing techniques. As a consequence, the solution processing of organic compounds, amorphous Si (a-Si), or ZnO-based semiconductors is all receiving significant attention. Zinc oxide is emerging as a promising candidate for thin film transistors (TFTs). There are a number of reasons for this: the raw materials are cheap and abundant; ZnO is nontoxic; it has excellent optical transparency; and this semiconductor has a high carrier mobility compared with a-Si or organic semiconductors. Zinc oxide also has the potential for low temperature processing.[1]

Currently, devices formed from solution-processed ZnO show inferior electrical properties and poor stability compared with those based on material deposited by thermal evaporation. It is widely known that a combination of additional materials, annealing, or post-deposition processing at high temperature is effective at improving transistor performance. For example, Kwack and W.-S. Choi[2] and Kim *et al.*[3] have reported solution-processed Zinc tin oxide (ZTO) TFTs with carrier mobilities of 4.9 and 6.0 cm^2/Vs using a high temperature annealing processes at 300 °C and 500 °C, respectively. Much research is now focused on post-deposition processing as part of an effort to keep the temperature below 150 °C. Indium zinc oxide (IZO) TFTs have achieved a mobility of 1.8 cm^2/Vs by using high-pressure annealing (HPA) following thermal annealing at 220 °C.[4] Similarly, UV light irradiation[5] and microwave-assisted annealing[6] have been adopted as useful post-deposition processes. Various passivation layers have also been used to reduce the effects of environmental factors, which lead to poor device stability.[7,8]

The effects of hydrogen exposure on ZnO thin films deposited by sputtering or pulse laser deposition (PLD) have also been noted.[9–11] In many instances, this can result in improved device performance. It has been reported that the incorporation of hydrogen in the sputtering gas enhances the carrier mobility. This is thought to result from an elimination of weakly-bound oxygen species, such as -CO_3, -OH, or adsorbed O_2 on the surface of the films.[12] Hydrogen treatment is already established as an important passivation process for Si-based transistors, where it is used to reduce significantly the density of interface traps.[13] There are limited studies on the effects of hydrogen on solution-processed ZnO thin films and devices. Here, we examine the results of hydrogen plasma treatment on the electrical behavior of solution-processed ZnO TFTs. An atmospheric plasma treatment has been used, which should ultimately lead to lower manufacturing costs.

II. EXPERIMENT

Bottom-gate, top-contact TFT structures were fabricated as shown in Figure 1. A p-doped Si substrate served as the gate electrode, while a 100 nm thick layer of SiO_2, grown by thermal oxidation, was used as the gate insulator. Before coating, the SiO_2 surface was treated with an UV ozone plasma for 5 min, which resulted in a hydrophilic surface. Zinc hydroxide was synthesized from zinc nitrate, $Zn(NO_3)_2$ (Duksan, 95%, used without further purification).[14] Carbonate-free sodium hydroxide, NaOH, solution was

a)Author to whom correspondence should be addressed. Electronic mail: m.c.petty@durham.ac.uk

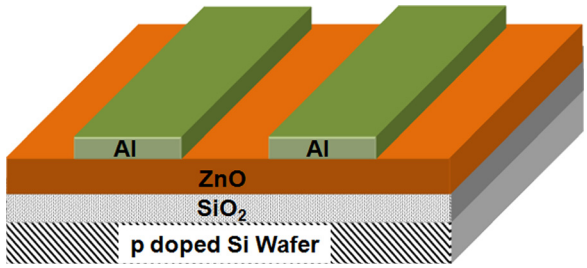

FIG. 1. Schematic diagram of the bottom-gate, top-contact ZnO TFT structure.

prepared from the supernatant in a saturated NaOH solution. To synthesize $Zn(OH)_2$, $Zn(NO_3)_2$ (49.8 g) was dissolved in de-ionized water (900 ml); it was then mixed with 600 ml of carbonate-free NaOH solution (~2.4 M). The clear solution was placed into an oil bath at 50 °C for 120 min. The resulting white precipitate ($Zn(OH)_2$) was filtered, and washed in de-ionized water three times. Finally, $Zn(OH)_2$ powder was obtained after further washing the filtered material in methanol and drying at room temperature. The maximum solubility of our $Zn(OH)_2$ was approximately 5% in ammonia water. The solution was spin coated onto the Si/SiO_2 substrates at 3000 rpm for 30 s, and subsequently baked at 140 °C for 30 min in air. Following deposition, the films were treated using an atmospheric cold plasma system (FemtoScience, AP100) with hydrogen gas for 10, 15, and 30 min at an RF power of 100 W. No bias was applied to the samples during this process. The argon and hydrogen flow rates to generate the plasma were 5 l/min and 2 sccm (standard cubic centimeters per minute), respectively. It was estimated that 30 min exposure to the plasma produced a temperature rise in our thin films of less than 50 °C. Finally, aluminium source (S) and drain (D) electrodes (80 nm in thickness) were defined by thermal evaporation through a shadow mask, under a vacuum of approximately 5×10^{-6} mbar; the channel length (L) and width (W) were 95 μm and 1660 μm, respectively. Electrical characterization of the transistors, in air, was undertaken in the dark using a Keithley 4200-SCS measurement system.

III. RESULTS AND DISCUSSION

Figure 2 shows the transfer characteristics of the ZnO TFTs as a function of hydrogen plasma treatment time. The drain-to-source voltage, V_{DS}, was fixed at 50 V, while the gate voltage, V_G, was swept from −10 V to 70 V and then back to −10 V at a scan rate of approximately 0.5 V/s. In the saturation region, the drain current, $I_{DS(sat)}$, can be expressed by

$$I_{DS(sat)} = \frac{WC_i}{2L}\mu(V_G - V_{TH})^2, \quad (1)$$

where C_i is the gate capacitance per unit area, V_{TH} is the transistor threshold voltage, and μ is the field effect mobility. For the devices shown in Fig. 2, the ratio of the channel width to length W/L = 17.5 and $C_i = 3.45 \times 10^{-8}$ F/cm^2. The values of μ and V_{TH} can be extracted from the slope of the forward scan and x-intercept, respectively, of a plot of $(I_{DS})^{1/2}$

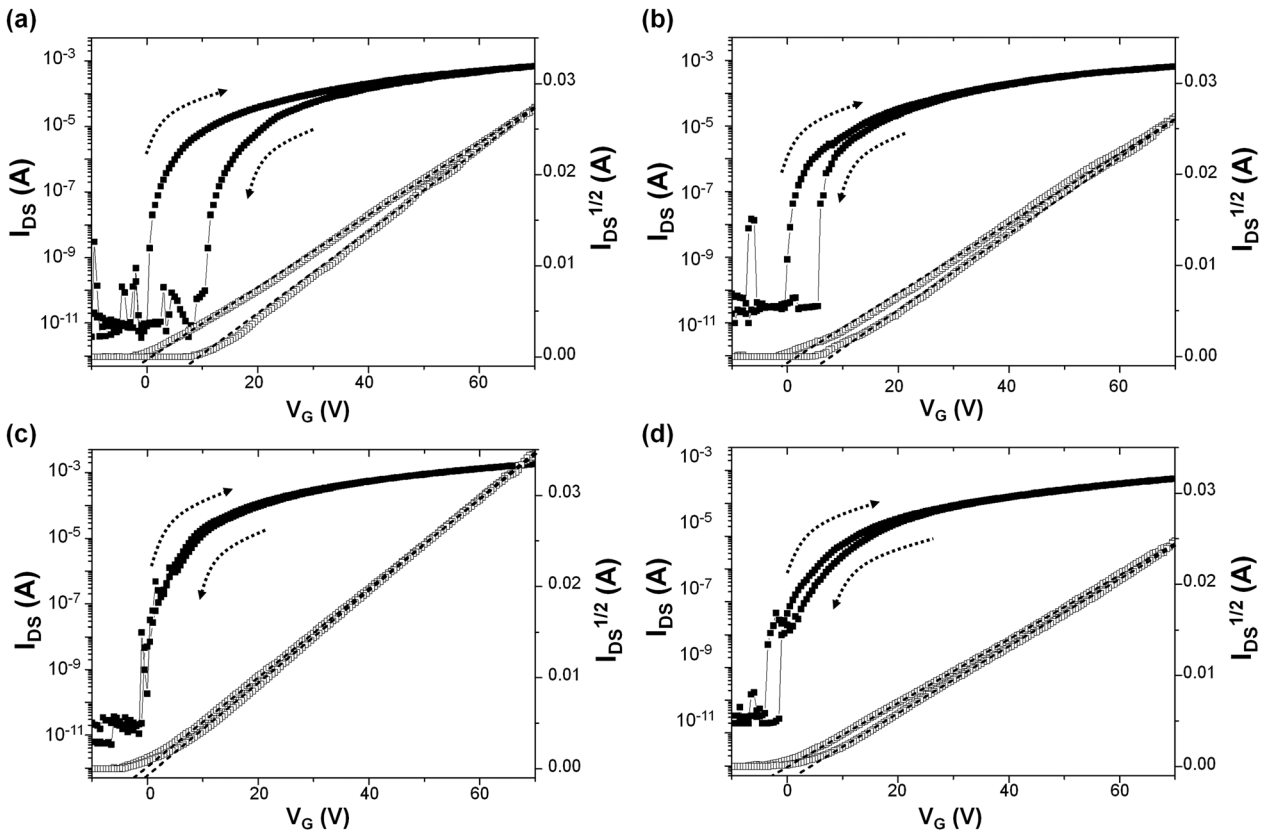

FIG. 2. Transfer characteristics (I_{DS}-V_G curve—full symbols) in the saturation region (V_{DS} = 50 V) of (a) reference, (b) 10 min, (c) 15 min, and (d) 30 min plasma treated ZnO TFTs. For each set of data, plots of $I_{DS}^{1/2}$ versus V_{DS} are also shown (open symbols).

versus V_G. These plots are shown alongside their respective transfer curves in Fig. 2.

From the data shown in Fig. 2, the values of V_{TH} and on/off ratio (the off current is defined as the value of I_{DS} at $V_{GS} = -10$ V and the on current is defined as the value of I_{DS} at $V_{GS} = 70$ V) for the un-treated ZnO TFTs are -2.1 V (by extrapolating the forward scan of $(I_{DS})^{1/2}$ versus V_G) and $\sim 10^7$, while the corresponding figures after 15 min of hydrogen plasma treatment are -5.1 V (also from the forward scan) and $\sim 10^7$. The untreated (reference) ZnO TFT exhibits a large hysteresis with a significant V_{TH} shift between the forward and reverse V_G scans. Following plasma treatment, this hysteresis is reduced significantly and the device mobility is enhanced. For example, the mobility in the saturation region is increased from 0.5 cm^2/Vs to 1.4 cm^2/Vs after hydrogen plasma treatment for 15 min, which appears to be about the optimum exposure time.

Figures 3(a)–3(d) reveal the dependence of the drain-source current (I_{DS}) on the drain-source voltage (V_{DS}) (output characteristics) for the ZnO TFTs after different hydrogen plasma treatment times; V_G was varied from 0 V to 50 V, in 10 V increments. All devices show typical n-channel operation. Good electrical contact between the aluminum S-D electrodes and ZnO is achieved irrespective of hydrogen plasma treatment time, as evidenced by the linearity at low V_{DS}. In each case, the value of the channel resistance in the transistor on state ($R_{DS,ON}$, $V_G = 50$ V) is approximately 2 kΩ. In addition, ZnO TFTs treated with the hydrogen plasma for 15 min exhibit higher saturation currents than untreated ZnO TFTs. This leads to the higher mobility value noted above.

To investigate the electrical stability of our ZnO TFTs, the transfer characteristics were re-measured over time. Figures 4(a)–4(d) show I_{DS} versus V_G curves as a function of hydrogen plasma treatment time at a fixed V_{DS} of 50 V. The V_G sweep was repeated four times, consecutively (~0.5 V/s). One interesting result from this experiment is that the large positive shift of V_{TH} (~17 V) and hysteresis in the reference device can both be largely eliminated by appropriate hydrogen plasma treatment; again the optimum plasma processing time is 15 min (Fig. 4(c)). We have also repeated these measurements after 30 days, using the same devices stored in air. The results are depicted in Figures 5(a)–5(d). The trends of the sets of data are quite similar to those shown in Fig. 4. Data extracted from Figs. 4 and 5 are re-plotted in Figure 6 to reveal changes in the important device characteristics as a function of plasma treatment time and measurement sequence: Fig. 6(a)—threshold voltage; Fig. 6(b) hysteresis (difference in V_{TH}) between forward and reverse voltage scans ($V_{THF} - V_{THR}$); and Fig. 6(c)—field effect carrier mobility.

The subthreshold swing (SS) for our devices can be related to the interface trap density, D_{it}, by the expression[15]

$$SS = \frac{qk_BT(N_{ss}t_{ch} + D_{it})}{C_i \log(e)}, \tag{2}$$

where N_{ss} is the density of bulk traps and t_{ch} is the thickness of the channel layer. Table I lists the values of SS and D_{it} obtained from the transfer characteristics shown in Figs. 4 and 5. The calculations were based on the assumption that $N_{SS}t_{ch} \ll D_{it}$. Figures are given from the first measurement of each device for different plasma processing times (1st set of data from Fig. 4, measurement sequence 1) and compared with the data measured from the 3rd scan following 30 days storage in air (3rd set of data from Fig. 5, measurement sequence 7). In each case, the value of SS was obtained from the forward scan in the respective transfer characteristic. It is evident from Table I that (i) for each device, D_{it} does not change very much over a period of

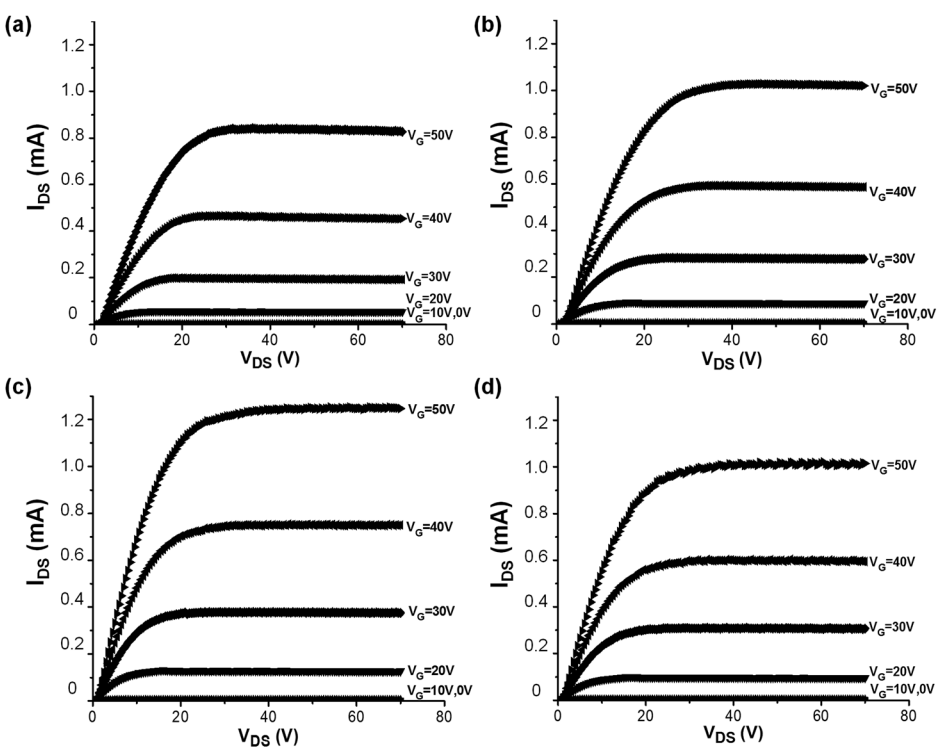

FIG. 3. Output characteristics ($I_{DS} - V_{DS}$ curve) of (a) reference, (b) 10 min, (c) 15 min, and (d) 30 min plasma treated ZnO TFTs.

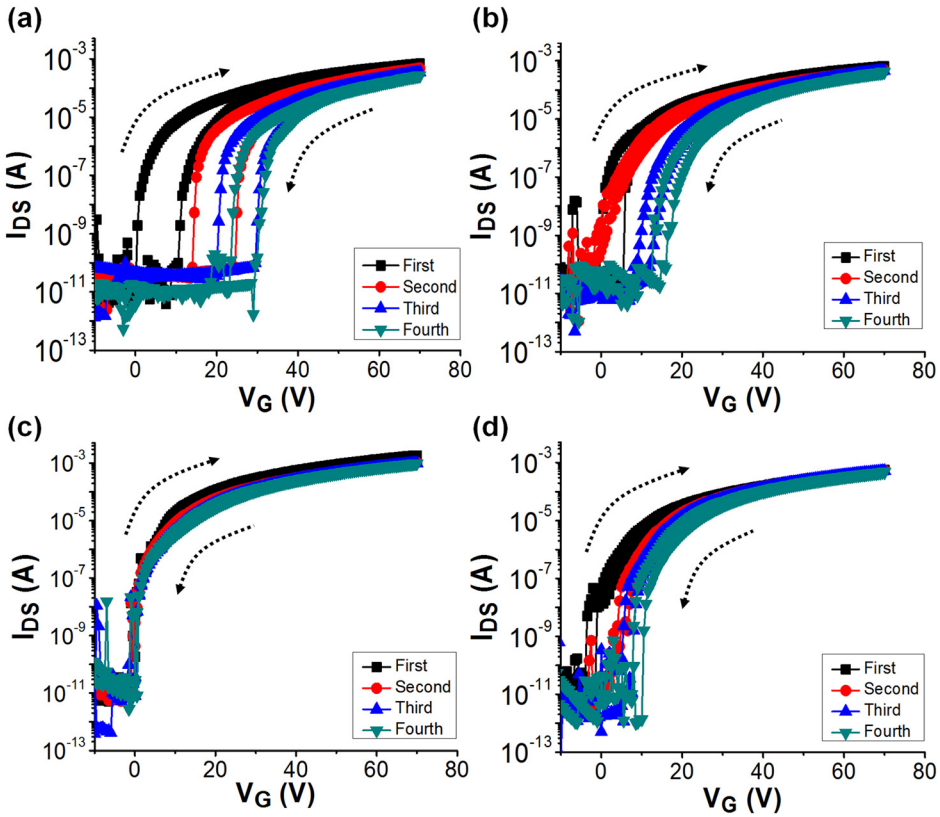

FIG. 4. Transfer characteristics of ZnO TFTs treated with hydrogen plasma for (a) 0 min, (b) 10 min, (c) 15 min, and (d) 30 min as a function of measurement sequence.

time and (ii) D_{it} is minimized for the device that had been subjected to plasma processing for 15 min.

The key observations from our experiments can be summarized as follows:

(i) the hydrogen plasma treatment can reduce significantly the hysteresis in the transfer characteristics of our TFTs;
(ii) the plasma treatment can enhance the field effect mobility;
(iii) the plasma treatment virtually eliminates the positive voltage shift in V_{TH} with repeated measurements; and
(iv) there is an optimum plasma treatment time, approximately 15 min in our study.

A further phenomenon is the slight negative shift in V_{TH} (−2.1 V to −5.1 V) following plasma treatment for 15 min, which is also seen in the reference device on exposure to air for a prolonged time (−2.1 V to −5.7 V).

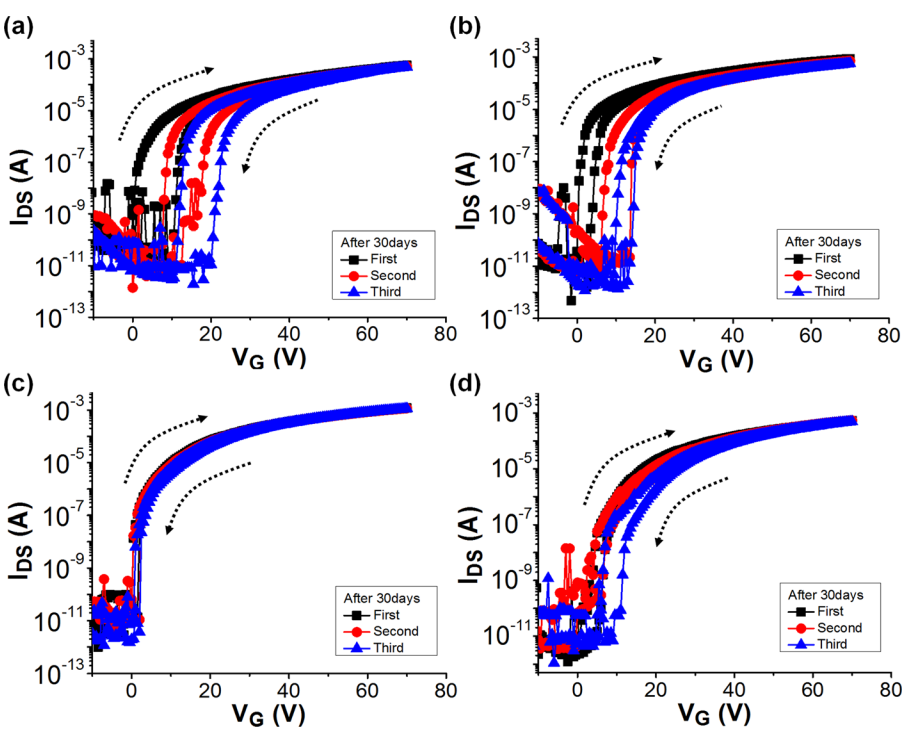

FIG. 5. Changes in the transfer characteristics of ZnO TFTs after 30 days.

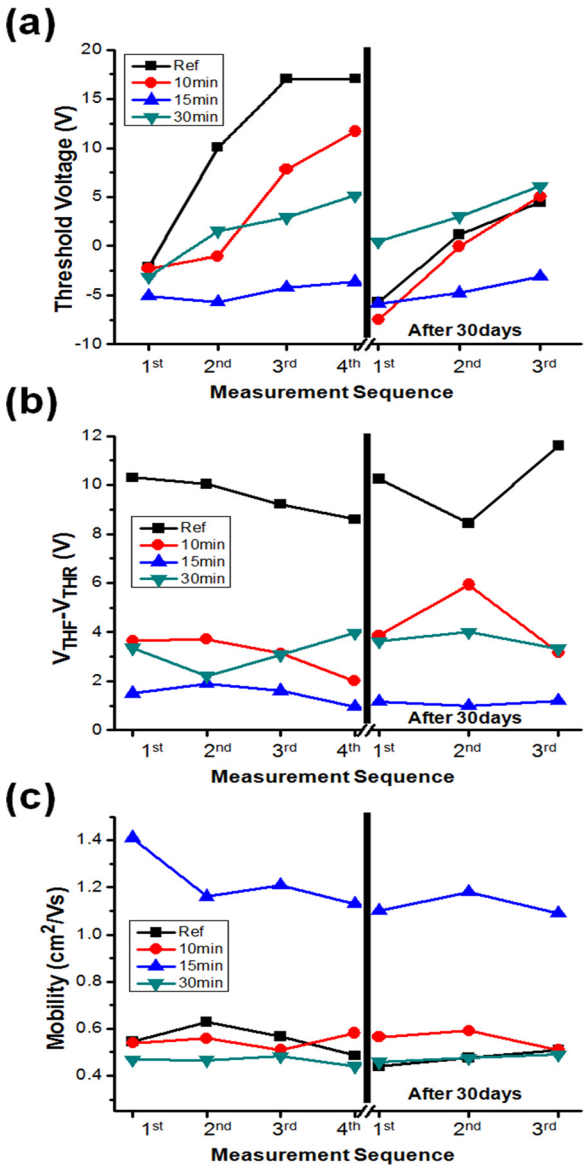

FIG. 6. Comparison of changes in the (a) V_{TH}, (b) the V_{TH} difference between forward and reverse scans ($V_{THF} - V_{THR}$), and (c) mobility of ZnO TFTs as a function of the measurement sequence for the various plasma treatment times.

Environmental effects are important factors in determining the stability of many TFTs. The adsorption and absorption of molecules, such as oxygen or water, can degrade the device performance. This problem is exacerbated by long exposure times to the atmosphere.[16,17] Several studies have investigated the use of various passivation methods to improve the TFT stability.[16,18] Following 30 days exposure to air, the threshold voltage of our reference device shifts in the negative V_G direction, from −2.1 V to −5.7 V. However, after 15 min of hydrogen plasma treatment, the corresponding change is from −5.1 V to −5.6 V, as shown in Fig. 6(a). These results can be explained by the effect of water molecules present in the environment. The ZnO active layer used in this study is likely to contain a relatively large number of OH groups, compared with ZnO films fabricated at high temperatures. While the device is exposed to the atmosphere, OH groups at the ZnO/SiO_2 interface interact with positively charged water molecules, leading to the formation of a region of electron accumulation. Therefore, we suggest that the shift of V_{TH} in the negative direction for the reference device after 30 days can be attributed to the attraction between water molecules in the air and OH groups in the film according to the reaction

$$H_2O \rightarrow H_2O^+ (ad) + e^-. \quad (3)$$

After the transfer characteristic had been measured four times, the threshold voltage for the reference TFT increases significantly, as noted previously, by about 17 V. This positive shift is reversible, with V_{TH} almost returning to its initial value after 30 days, but, if the measurements were re-started, the positive shift in V_{TH} is again observed. Exposure to the hydrogen plasma for 15 min virtually eliminates this positive shift in V_{TH}. Moreover, as shown in Fig. 6(b), the average difference between the forward and reverse scans is approximately 1 V for the 15 min plasma treated ZnO TFTs, which is very small compared with the reference device, where the hysteresis exceeds 10 V. These values do not vary very much with time.

The hysteresis and V_{TH} shift in our reference TFTs can also originate from unreacted OH groups in the ZnO film. On application of a positive V_G for the reference TFT, the OH groups in the vicinity of the semiconductor/insulator interface can trap electrons, causing a lowering of the effective gate bias and resulting in a smaller current flowing through the channel. Consequently, a larger positive voltage is required for the device to turn on. Jeong *et al.*[19] have reported that excess OH groups can be removed in the form of H_2O by heat treatment at 500 °C, leaving oxygen vacancies. The reaction is

$$Zn\cdots OH + H^+ \rightarrow Zn^+ + H_2O \uparrow . \quad (4)$$

We suggest that our hydrogen plasma treatment produces similar effects. The plasma processing is therefore a promising method for enhancing dehydroxylation/dehydration reactions, which could lead to a low temperature process, and resulting in TFTs with excellent electrical properties. It has also been noted that oxygen vacancies, which act as n-type donors, play an important role as a source of charge carriers in oxide semiconductors.[20] The carrier trapping associated

TABLE I. Subthreshold swing (SS) and interface trap density (D_{it}) for ZnO TFTs treated with hydrogen plasma for different times.

Plasma treatment time	0 min		10 min		15 min		30 min	
Measurement sequence	1st	7th	1st	7th	1st	7th	1st	7th
SS (V/decade)	0.48	0.44	0.29	0.25	0.19	0.16	0.34	0.30
D_{it} ($eV^{-1}cm^{-2}$)	1.91×10^{12}	1.75×10^{12}	1.15×10^{12}	9.94×10^{11}	7.56×10^{11}	6.36×10^{11}	1.35×10^{12}	1.19×10^{12}

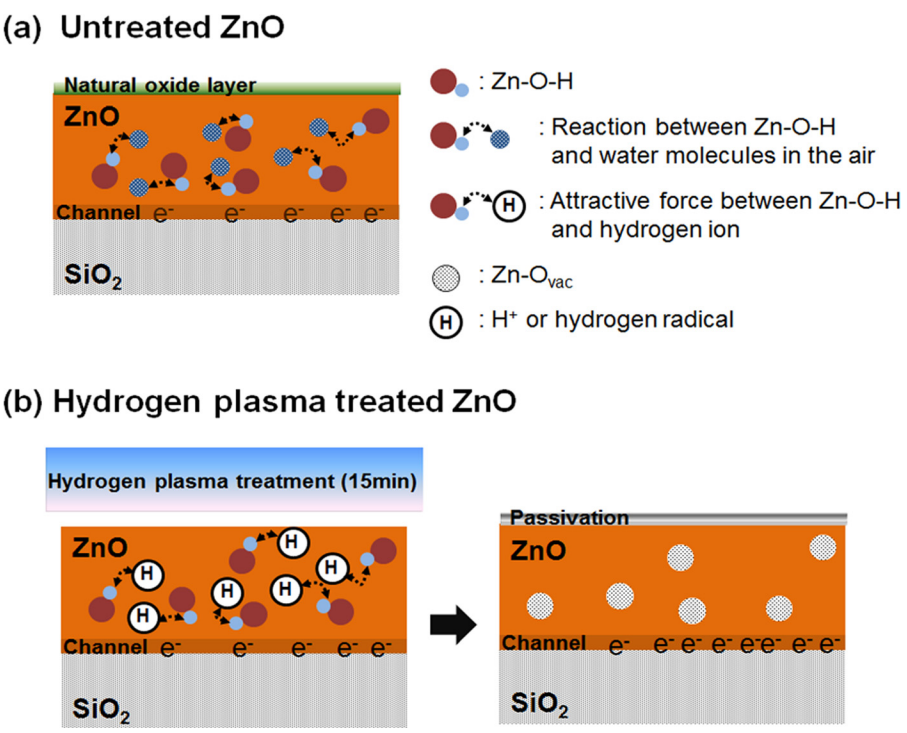

FIG. 7. Model for the interaction between ZnO and hydrogen plasma.

with the polar OH groups will also reduce the electron mobility in the TFTs.[6,21] The negligible hysteresis and small V_{TH} shift in the transfer characteristics after 30 days for the 15 min hydrogen plasma treated TFTs indicate that the hydrogen plasma treatment might also passivate the semiconductor/insulator interface, helping to prevent degradation of the electrical properties when the devices are exposed to air for a long time. This is confirmed by the relatively low value of D_{it} measured from the subthreshold swing following 15 min of plasma processing (Table I).

Figure 7 shows a model based on our experimental observations. This indicates the possible interactions occurring between Zn-O-H and the hydrogen ions in the plasma. When a ZnO film is formed by solution processing, a high density of unstable Zn-O-H may be present throughout the film, as depicted in Fig. 7(a). The OH groups act as electron trapping sites, leading to a decrease in the effective number of carriers and to a reduction in the carrier mobility. This accounts for the large hysteresis in the transfer characteristics of our reference TFTs. However, after hydrogen plasma treatment, the unstable Zn-O-H groups react with hydrogen ions, releasing H_2O and creating oxygen vacancies. Although the devices are not intentionally heated during exposure to the plasma, we suggest that there is sufficient energy available during the processing to remove any water molecules from the ZnO layer. As no bias is applied to our samples during the plasma treatment, we suggest that the plasma hydrogenation processes occur via a diffusion mechanism. In our experiments, the optimum plasma processing time is 15 min. We propose that longer exposures lead to accumulation of hydrogen within the TFT structure, resulting in deterioration of the electrical performance of the transistor.

IV. CONCLUSION

Zinc oxide thin film transistors have been prepared by solution processing and low temperature annealing at 140 °C. The devices were subjected to a post-deposition atmospheric hydrogen plasma treatment, which appeared to influence the dehydroxylation/dehydration of the solution-processed ZnO films. Two benefits were evident: an improvement in the transistor electrical properties and a longer term passivation effect. Devices with field effect mobilities of 1.4 cm^2/Vs, an on/off ratio of 10^7, a threshold voltage of −5 V, minimal hysteresis in the transfer characteristics, and good stability over several weeks' exposure to an air ambient were achieved. These results suggest that ZnO transistors with useful electrical performance can be manufactured by solution processing followed by an appropriate, low-temperature post-deposition processing.

ACKNOWLEDGMENTS

This work was supported by the Industrial Strategic Technology Development Program (10041808, Synthesis of Oxide Semiconductor and Insulator Ink Materials and Process Development for Printed Backplane of Flexible Displays Processed Below 150 °C) funded by the Ministry of Knowledge Economy (MKE, Korea).

[1]P. M. C. Barquinha, E. M. C. Fortunato, C. M. B. G. Pimentel, A. M. F. Goncalves, A. J. S. Marques, L. M. N. Pereira, and R. F. P. Martins, Adv. Mater. **17**, 590 (2005).
[2]Y.-J. Kwack and W.-S. Choi, IEEE Electron Device Lett. **34**, 78 (2013).
[3]Y. J. Kim, B. S. Yang, S. Oh, S. J. Han, H. W. Lee, J. Heo, J. K. Jeong, and H. J. Kim, ACS Appl. Mater. Interfaces **5**(8), 3255 (2013).
[4]Y. S. Rim, W. H. Jeong, D. L. Kim, H. S. Lim, K. M. Kim, and H. J. Kim, J. Mater. Chem. **22**(25), 12491 (2012).
[5]H. Faber, Y.-H. Lin, S. Rossbauer, and T. D. Anthopoulos, Appl. Phys. Lett. **102**, 193516 (2013).
[6]T. Jun, K. Song, Y. Jeong, K. Woo, D. Kim, C. Bae, and J. Moon, J. Mater. Chem. **21**(4), 1102 (2011).
[7]S.-H. Choi, J.-H. Jang, J.-J. Kim, and M.-K. Han, IEEE Electron Device Lett. **33**, 381 (2012).
[8]K. Nomura, T. Kamiya, and H. Hosono, Thin Solid Films **520**, 3778 (2012).

[9]A. Singh, S. Chaudhary, and D. K. Pandya, Appl. Phys. Lett. **102**, 172106 (2013).
[10]A. Kronenberger, A. Polity, D. M. Hofmann, B. K. M. A. Schleife, and F. Bechstedt, Phys. Rev. B **86**, 115334 (2012).
[11]S. W. Tsao, T. C. Chang, S. Y. Huang, M. C. Chen, S. C. Chen, C. T. Tsai, Y. J. Kuo, Y. C. Chen, and W. C. Wu, Solid-State Electron. **54**, 1497 (2010).
[12]X. T. Hao, F. R. Zhu, K. S. Ong, and L. W. Tan, Semicond. Sci. Technol. **21**, 48 (2006).
[13]J. Lee, K. Cheng, Z. Chen, K. Hess, J. W. Lyding, Y. K. Kim, H. S. Lee, Y. W. Kim, and K. P. Suh, IEEE Electron Device Lett. **21**, 221 (2000).
[14]H. Kim, J. Hwang, and M. Lee, Korea patent application 10-2013-0164867 Dec. 27, 2013.
[15]D. W. Greve, *Field Effect Devices and Applications: Devices for Portable, Low-Power, and Imaging Systems*, 1st ed. (Prentice Hall, Englewood Cliffs, NJ, 1988), p. 87.
[16]J. K. Jeong, H. W. Yang, J. H. Jeong, Y.-G. Mo, and H. D. Kim, Appl. Phys. Lett. **93**(12), 123508 (2008).
[17]Y. Li, F. D. Valle, M. Simonnet, I. Yamada, and J.-J. Delaunay, Appl. Phys. Lett. **94**(2), 023110 (2009).
[18]X. Xu, L. Feng, S. He, Y. Jin, and X. Guo, IEEE Electron Device Lett. **33**(10), 1420 (2012).
[19]Y. Jeong, C. Bae, D. Kim, K. Song, K. Woo, H. Shin, G. Cao, and J. Moon, ACS Appl. Mater. Interfaces **2**, 611 (2010).
[20]J. Schoenes, K. Kanazawa, and E. Kay, J. Appl. Phys. **48**, 2537 (1977).
[21]N. Huby, S. Ferrari, E. Guziewicz, M. Godlewski, and V. Osinniy, Appl. Phys. Lett. **92**, 023502 (2008).